American Mineralogist, Volume 72, pages 1176–1189, 1987

Ashcroftine, ca. $K_{10}Na_{10}(Y,Ca)_{24}(OH)_4(CO_3)_{16}(Si_{56}O_{140})\cdot 16H_2O$, a structure with enormous polyanions

Paul Brian Moore
Department of the Geophysical Sciences, The University of Chicago, Chicago, Illinios 60637, U.S.A.
Pradip K. Sen Gupta
Department of Geology, Memphis State University, Memphis, Tennessee 38152, U.S.A.
Elmer O. Schlemper
Department of Chemistry, University of Missouri, Columbia, Missouri 65211, U.S.A.
Stefano Merlino
Dipartimento di Scienze della Terra, Università di Pisa, 56100 Pisa, Italy

Abstract

The elephantine crystal structure of ashcroftine, end member ca. $K_{10}Na_{10}(Y,Ca)_{24}(OH)_4(CO_3)_{16}(Si_{56}O_{140})\cdot 16H_2O$ has been independently investigated (Moore, Sen Gupta, Schlemper = MSS; Merlino = M) in two laboratories. Type material from Narsarsuk, Greenland, afforded crystals for both studies. The ashcroftine average structure is tetragonal holosymmetric, space group $I4/m\ 2/m\ 2/m$, $a = 23.994(6)$, $c = 17.512(5)$ (MSS) and $a = 24.039(6)$, $c = 17.538(8)$ (M), $Z = 2$. $R = 0.058$ for 1774 independent F_o values (MSS) and 0.060 for 2276 F_o values (M).

The structure is based on at least 39 atoms in the asymmetric unit. Of these, 27 are ordered and make up the $[K_8Na_2Y_{24}(OH)_4(CO_3)_{16}(Si_{48}O_{128})\cdot 10H_2O]^{18-}$ fraction. The underlying polyanion is a giant $[Si_{48}O_{128}]$ ball whose connections define a polyhedron, hence a *balosilicate.* It has point symmetry $(4/m\ 2/m\ 2/m)$, a near subgroup of $(4/m\ \bar{3}\ 2/m)$ found for the related truncated cuboctahedron, an Archimedean solid. Breaks in the ball admit an extensive circumjacent disordered region and together define the $^1_\infty[Si_{56}O_{140}]$ tubular inosilicate with channels and bulges, oriented parallel to [001]. All terminal oxygens point outside, away from the central channel. The ordered carbonate fraction defines, among other things, ordered $[Na(CO_3)_4]$ clusters. The entire ordered region is called the *curd.*

The large balls are encrusted with a border region, or *limbus,* with Y–O, Na–O, and K–O bonds. The disordered region of 12 atoms in the asymmetric unit, or the *whey,* consists of partly occupied T(D) = (Si,B), Si; Na(D), K(D), and ϕ ($\phi = O^{2-}$, OH^-, H_2O) sites.

It is proposed that the $[Si_{48}]$ core constituted the template for ashcroftine's growth and that other related monsters may occur in a similar paragenesis.

Introduction

Gordon (1924) initiated the curious history of the exotic ashcroftine. It is appropriate to give a brief review of the discovery and subsequent studies on the species that, as we shall see, possesses a most remarkable and unusual crystal structure. Gordon christened it *kalithomsonite,* and he found it in "pocket K," one-half meter below the surface. This site is near the famous mineral locality Narsarsuk, which is situated 45 km northeast from Julianehaab, in southwestern Greenland. Most of the classic mineral occurrences of Steenstrup, Flink, and Gordon were confined within a kilometer-wide zone of augite-syenite. The exotic minerals occur within small, irregular pegmatitic vugs. The pegmatites are composed of coarse feldspar crystals, aegirine, some arfvedsonite and eudialyte of which many tons were collected.

"Pocket K" was a vug 15 cm in greatest dimension. From the augite-syenite rock inward, Gordon noted the sequence of precipitation or paragenesis from oldest to youngest: aegirine + orthoclase + zinnwaldite + graphite → etched quartz crystals → elpidite + albite → calcite → kalithomsonite. The kalithomsonite occurred as pink aggregates of fibers that completely filled the cavity remaining in the vug. Despite much digging circumjacent to the pocket, no other pockets with similar contents were discovered.

Chemical analysis by Whitfield reported in Gordon (1924) is repeated in Table 1. The small kalithomsonite crystals measuring up to 0.25 × 4 mm in dimension had some peculiar properties. Gordon noted cleavages $a(100)$ less perfect, $b(010)$ perfect, $c(001)$ imperfect; $\alpha = 1.535$, $\beta = 1.537$, $\gamma = 1.545$, $X = b$, $Y = a$, $Z = c$; and he emphasized the optical differences from normal thomsonite ($X = a$, $Y = c$, $Z = b$, $\alpha = 1.535$, $\beta = 1.531$ [sic],

0003–004X/87/1112–1176$02.00

$\gamma = 1.541$, according to Gordon). Based on the Whitfield analysis, he proposed a formula close to KNa(Ca,Mg,-Mn)$[Al_4Si_5O_{18}]\cdot 10H_2O$.

Hey and Bannister (1933), in the course of studies on zeolites, re-examined kalithomsonite. They expressed doubts based on the published optical data that kalithomsonite was a thomsonite at all. Furthermore, the $a(100)$ and $b(010)$ cleavage planes appeared equally developed, and no difference was noted between α and β. X-ray single-crystal study revealed an enormous unit cell, the largest then known for an inorganic substance, $a = 34.04(5)$, $c = 17.49(5)$ [Note: $a/\sqrt{2} = 24.07$ Å]. Other salient details: cell contents $40[KNa(Ca,Mg,Mn)Al_4Si_5O_{18}\cdot 8H_2O]$, tentative space group $D_{4h}^{14} = P4_2/mnm$, $\omega = 1.536$, $\epsilon = 1.545$, small bundles bounded by cleavages $a\{100\}$, $c\{001\}$, specific gravity 2.61(5). Thus, kalithomsonite was an entirely new species, named *ashcroftine* after Mr. Frederick Noel Ashcroft, who presented large gifts of zeolites to the cabinet of the British Museum of Natural History.

There the matter stood until Moore et al. (1969) attempted the crystal structure of ashcroftine in earnest, but the Patterson synthesis could not possibly be interpreted according to the then-accepted composition, so recourse was made to ARL electron-microprobe scans. It was discovered that only trace Al was present; in its stead there was actually Y with minor amounts of lanthanides. In Table 1, we accepted Y_2O_3 in lieu of the Al_2O_3 of Gordon (1924). The results: $a = 24.044(4)$, $c = 17.553(8)$ Å, space group *I*4/*mmm*, *I*4*mm*, *I*422 or $I\bar{4}m2$, proposed formula $KNaCaY_2Si_6O_{12}(OH)_{10}\cdot 4H_2O$, $Z = 16$. Ashcroftine was therefore proposed to be not a zeolite but possibly related to lovozerite (since both species are found associated with nepheline syenites), enthusiasm for the difficult structure problem at hand was lost, and further study was abandoned.

The ashcroftine saga continued. In 1973, Merlino received the vial of ashcroftine from Moore, who initially received a portion of Gordon's *type material* from the U.S. National Museum of Natural History (NMNH 95320). Sen Gupta, unaware of the other work, received crystals from the British Museum of Natural History (no. BM 1924,867; Narsarsuk, Greenland). These samples came from the same batch collected by Gordon. Moore was called on the scene when an impasse was reached in the structure determination by Sen Gupta. A seemingly routine problem ballooned into one of considerable complexity. When it was discovered that Merlino also rejuvenated the problem, we joined forces. The present contribution is a combination of two relatively independent studies, and results from both are given. For exceedingly complicated structures, presentation of two independent sets of data has advantages and lessens the phantasmagoria that occasionally creep into study of such monsters.

We show that ashcroftine is, for an average structure, tetragonal holosymmetric, space group *I*4/*m* 2/*m* 2/*m*, $a = 24.02$, $c = 17.52$ Å, $Z = 2$ for a formula unit ca. $Na_{10}K_{10}Y_{24}(OH)_4(CO_3)_{16}(Si_{56}O_{140})\cdot 16H_2O$. Essential carbonate groups earlier unreported (but probably incorporated into the water analysis of Whitfield) were uncovered, as well as a disordered enormous $^1_\infty[Si_{56}O_{140}]$ tube, whose ordered bulbous part is in fact derived from the giant cage $[Si_{48}\phi_{120}]$ that is the Archimedean semiregular truncated cuboctahedron with Si at the vertices and ϕ (anions) at midpoints of the edges, with 48 additional terminal ϕ bonded to the Si atoms and protruding outward.

TABLE 1. Ashcroftine chemical analysis and interpretation

	1*	2*	3*	4*	5*
Na_2O	3.62	3.62	3.55	4.38	3.93
K_2O	5.65	5.65	6.33	6.04	5.97
MgO	0.87	0.87	—	—	—
CaO	5.72	5.72	2.28	2.53	—
MnO	0.79	0.79	—	—	—
B_2O_3	—	—	—	1.90	—
Al_2O_3	26.61	—	—	—	—
Y_2O_3	—	26.61	31.17	30.40	34.38
CO_2	—	7.2	9.29	9.22	8.93
SiO_2	38.09	38.09	42.95	40.78	42.68
H_2O (>100 °C)	12.00	4.8	4.43	4.75	4.11
H_2O (<100 °C)	6.40	6.40	—	—	—
Total	99.75	99.75	100.00	100.00	100.00

* (1) Whitfield in Gordon (1924). (2) Column 1 with Al_2O_3 reckoned as Y_2O_3. No Al_2O_3 was detected by electron-microprobe analysis. The CO_2 content was determined by vapor-pressure measurement, in a procedure discussed by Harris (1981). It was subtracted from H_2O (>100 °C) determined by Whitfield in Gordon (1924), assuming that upon ignition both CO_2 and H_2O were lost. (3) Calculated composition based on site occupancies in Table 3 and the MSS formula in the section on Chemical Composition. (4) The same, but for M. (5) For $K_{10}Na_{10}Y_{24}(OH)_4(CO_3)_{16}(Si_{56}O_{140})\cdot 16H_2O$.

The presence of (CO_3) groups presented problems in the chemical interpretation, and it was most desirable to determine the quantity of carbonate by independent means. A. T. Anderson volunteered to measure the concentration of CO_2 in a small ashcroftine crystal. The microdetermination, which employs a heating stage, cryopump, and vapor-pressure measurement, was announced by Harris (1981). The gas species were easily discriminated by their solid-vapor equilibria during sublimation of individual components.

Measurement of the single crystal gave $2.8(4) \times 10^{-6}$ cm^3 corresponding to a mass of $7.2(10) \times 10^{-6}$ g. Most CO_2 was lost between 550 and 1000 °C. The total mass of CO_2 lost below 1250 °C computed to 5.2×10^{-7} g. The crystal was reduced to a blebby mass.

The concentration of CO_2 is therefore 7.2(11) wt%. The proposed value for CO_2 based on site occupancies in Table 1 is 9.3 wt%, about 20% higher than the microdetermination, a not at all unreasonable difference for so small a crystal. In any event, CO_2 is clearly essential and firmly bonded in ashcroftine's crystal structure.

EXPERIMENTAL DETAILS

Acronyms for the two separate studies include MSS for Moore, Sen Gupta, and Schlemper; and M for Merlino. Crystals of ashcroftine are usually ten times as long as they are thick, of simple

TABLE 2. Experimental details for ashcroftine

	MSS	M
	(A) Crystal cell data	
a (Å)	23.994(6)	24.039(6)
c (Å)	17.512(5)	17.538(8)
Space group	$I4/m\ 2/m\ 2/m$	
Z	2	
Formula	End member ca. $Na_{10}K_{10}Y_{24}(OH)_4(CO_3)_{16}(Si_{56}O_{140})\cdot 16H_2O$	
ρ_{calc}* ($g\cdot cm^{-3}$)	2.60	
Specific gravity†	2.61(5)	
μ (cm^{-1})	77.89	—
	(B) Intensity measurements	
Crystal size (μm)	50 ($\parallel a_1$) × 100 ($\parallel a_2$) × 350 ($\parallel c$)	small, no absorption correction
Diffractometer	Enraf-Nonius CAD-4	Philips PW1100
Monochromator	Graphite	
Max (sin θ)/λ	0.60	0.70
Scan, deg per min	θ–2θ 2.0	θ–2θ 3.6
Base scan width (deg)	0.7–1.3	1.20
Background counts	Stationary, 20 s at beginning and end of scan	
Radiation	Mo$K\alpha$ (λ = 0.71069 Å)	
Measured intensities	2538	2535
Independent F_o	1774	2276 [$\geq 5\sigma[F_o)$]
	(C) Refinement of the structure	
R	0.058	0.060
	Unit weights	
Scattering factors	Neutral atoms (Ibers and Hamilton, 1974)	

* From average of MSS and M cell volumes and formula proposed.
† Hey and Bannister (1933).

tetragonal prismatic development, palest pink in color, and striated parallel to [001]. Table 2 summarizes the experimental details. In the MSS study, the space group $I4/mmm$ was initially assumed. In addition, the $N(z)$-test for presence or absence of symmetry centers (Howells et al., 1950) also supported the centric model. For cell-parameter refinement, 25 reflections of intermediate Bragg angle were selected. An empirical ψ-scan facilitated absorption correction, since the crystal possessed a relatively low average atomic number. The data were then adjusted for Lorentz and polarization factors, and the empirical absorption correction was applied. Symmetry-equivalent reflections were merged to provide a set of 1774 independent F_o values.

Solution of the structure proceeded at two stages. The heavier atoms (Y and K) were located by MULTAN (Main et al., 1977), and successive difference syntheses revealed all ordered non-H atoms in the asymmetric unit. Refinement employed full-matrix least-squares methods with the program SHELX–76 and was continued until no further changes in positional and anisotropic thermal parameters occurred. The second stage of structure determination mentioned above involved the disordered part of the structure and will be summarized later.

The approach and procedure of M was very similar. Least-squares fitting of 25 Bragg reflections led to cell parameters similar to MSS but about 0.2% higher. We have no explanation for this difference. Lorentz and polarization adjustments were made, but there was no absorption correction owing to the small and favorable shape of the crystal. The structure solution proceeded with the Patterson synthesis, which located the Y(1) and Y(2) atomic positions, followed by successive Fourier syntheses.

In both studies, unit weights were used throughout, and the scattering factors for neutral atoms and real and imaginary dispersion corrections were taken from Ibers and Hamilton (1974). Refinement minimized $\Sigma\, w(|F_o| - F_c|)^2$ where s^{-1} = unit weight. The conventional R index, where $R = (\Sigma\, \|F_o| - |F_c\|)/\Sigma\, F_o$ is given in Table 2 for both studies.

A comment on the disordered atoms is necessary, since these constituted by far the most difficult part of the structure study. Table 3, which lists the atomic coordinate parameters for ashcroftine from the two studies, is divided into two parts. The first section includes all atoms in the asymmetric unit that fully occupy their sites. These could be called the ordered atoms, but the term is ambiguous as it has many meanings. Since they do not exhibit any obvious pathological behavior, we call these 27 independent atoms the *healthy* atoms. In our designations, we include Si(1) to Si(3), O(1) to O(14), C(1), C(2), OH(1), OW(1), OW(2), Y(1), Y(2), K(1), K(2), and Na(1). The second section includes 12 independent atomic positions; these presented by far the greatest difficulties. All of them have the letter *D* affixed to their designations. One central problem was discriminating partly occupied cation sites from disordered water molecules. Here, all nearest and second-nearest bond distances and determination of coordination polyhedra were important clues toward the hopefully correct choice. Although we kept in frequent communication concerning the nature of these positions, the concord between the two studies is not nearly so evident as in the healthy atoms of the first section where most atom pairs are within their limits of estimated standard deviation. These we shall call the 12 *pathological* atoms. Note that M split T(1D) into both a contribution by Si and by B after he discovered a small B content (0.5–1.0%) in ashcroftine by semiquantitative spectrographic analysis. MSS, on the other hand, treated T(1D) and T(2D) as partly occupied Si sites. Doubtless the pathological atoms have a small but real contribution toward the parameter convergence for the entire structure, and possible other disordered atoms (particularly water molecules) in the large central ball were not located. Finally, MSS treated Y(1) and Y(2) as Y populations, whereas M included scattering curves for Y and complementary Ca in purported solid solution. Both models, which converged well, should have their differences manifested in the thermal-vibration ellipsoids.

We believe that beyond the 27 atoms in the healthy part of

TABLE 3. Ashcroftine atomic coordinates

			(Healthy part) MSS			M		
Atom	Occ.	Mul.	x	y	z	x	y	z
Si(1)	1.00	32	0.2414(1)	0.1510(1)	0.4128(2)	0.2417(1)	0.1513(1)	0.4127(2)
Si(2)	1.00	32	0.2697(2)	0.0635(1)	0.2945(2)	0.2696(1)	0.0637(1)	0.2940(2)
Si(3)	1.00	32	0.2188(2)	0.0630(1)	0.1339(2)	0.2186(1)	0.0631(1)	0.1338(2)
O(1)	1.00	32	0.2371(4)	0.0935(4)	0.3644(5)	0.2368(3)	0.0943(3)	0.3634(5)
O(2)	1.00	32	0.2235(4)	0.0619(4)	0.2264(5)	0.2247(4)	0.0622(4)	0.2256(5)
O(3)	1.00	32	0.3018(3)	0.1780(4)	0.4034(5)	0.3016(3)	0.1784(3)	0.4025(5)
O(4)	1.00	32	0.2682(4)	0.0970(4)	0.0958(5)	0.2684(4)	0.0961(3)	0.0950(5)
O(5)	1.00	32	0.3247(4)	0.0958(4)	0.2695(5)	0.3254(3)	0.0952(3)	0.2700(4)
O(6)	1.00	32	0.1595(4)	0.0875(5)	0.1160(8)	0.1591(4)	0.0885(5)	0.1153(9)
O(7)	1.00	16	0.1912(4)	0.1912	0.3848(6)	0.1905(3)	0.1905	0.3839(6)
O(8)	1.00	16	0.2297(6)	0.1322(5)	½	0.2293(5)	0.1320(5)	½
O(9)	1.00	16	0.2807(6)	0	0.3205(8)	0.2811(6)	0	0.3215(7)
O(10)	1.00	16	0.2200(7)	0	0.1033(8)	0.2189(7)	0	0.1014(8)
C(1)	1.00	16	0.4002(9)	0	0.1582(15)	0.4027(9)	0	0.1574(11)
O(11)	1.00	32	0.4261(5)	0.0469(5)	0.1713(7)	0.4271(4)	0.0468(4)	0.1698(7)
O(12)	1.00	16	0.3529(7)	0	0.1315(10)	0.3518(7)	0	0.1320(10)
C(2)	1.00	16	0.3709(11)	0.0923(10)	½	0.3709(8)	0.0919(8)	½
O(13)	1.00	32	0.3596(5)	0.0693(4)	0.4353(5)	0.3590(4)	0.0686(4)	0.4361(5)
O(14)	1.00	16	0.3932(6)	0.1411(6)	½	0.3944(5)	0.1398(5)	½
OH(1)	1.00	8	0.2473(5)	0.2473	½	0.2475(5)	0.2475	½
OW(1)	1.00	16	0.1264(7)	0.1264	0.2782(9)	0.1285(4)	0.1285	0.2784(6)
OW(2)	1.00	4	½	0	0	½	0	0
*Y(1)	1.00	32	0.3556(1)	0.1152(1)	0.1468(1)	0.3559(1)	0.1145(1)	0.1465(1)
*Y(2)	1.00	16	0.2679(1)	0.1618(1)	0	0.2677(1)	0.1616(1)	0
K(1)	1.00	8	0.2704(5)	0	½	0.2696(4)	0	½
K(2)	1.00	8	0.3057(4)	0	0	0.3055(4)	0	0
Na(1)	1.00	4	½	0	¼	½	0	¼

			(Pathological part) MSS				M		
Atom	Mul.	Occ.	x	y	z	Occ.	x	y	z
T(1D)	16	Si 0.38	0.1336(4)	0.1336	0.0622(8)	Si 0.20 B 0.52	0.1344(4)	0.1344	0.0675(8)
T(2D)	16	Si 0.39	0.0986(5)	0.0986	0.0905(11)	Si 0.28(2)	0.0986(5)	0.0986	0.0901(11)
K(1D)	16	0.30	0.2158(10)	0.2158	0.2057(21)	0.25	0.2146(9)	0.2146	0.2089(20)
Na(1D)	16	0.45	0.4181(10)	0	0.3924(15)	0.50	0.4210(10)	0	0.3946(16)
Na(2D)	16	0.28	0.3900(17)	0	0.3585(25)	0.50	0.3902(10)	0	0.3611(18)
Na(3D)	4	0.42	0	0	0	0.40(6)	0	0	0.0322(20)
ϕ(1D) OH^-	16	0.49	0.1859(9)	0.1859	0.0772(21)	OH^- 0.61(4)	0.1835(6)	0.1835	0.0746(13)
ϕ(2D) OH^-	16	0.30	0.0532(10)	0.0532	0.1270(26)	OH^- 0.28(2)	0.0545(22)	0.0545	0.1238(43)
ϕ(3D) H_2O	16	0.13	0.1441(37)	0.1086(41)	0	O^{2-} 0.31(6)	0.1426(30)	0.1124(28)	0
ϕ(4D) O^{2-}	8	0.54	0.0983(12)	0.0983	0	O^{2-} 0.63(8)	0.0948(15)	0.0948	0
ϕ(5D) H_2O	8	0.36	0.1036(29)	0	0	H_2O 0.66(10)	0.1099(28)	0	0
ϕ(6D) OH^-	8	0.50	0.1733(15)	0.1733	0	OH^- 0.49(10)	0.1776(24)	0.1776	0

Note: Estimated standard errors refer to the last digit. Occ. refers to fractional occupancy at a site; Mul. is number of equivalences in space group *I4/mmm*.

* In M, refined to Y(1) = 0.89(1)Y + 0.11Ca and Y(2) = 0.79(2)Y + 0.21 Ca. MSS employed only Y.

the structure, the inclusion of the 12 atoms in the pathological part leads to an *averaged* crystal structure at best. Most of the pathological atoms can be traced to the behavior of the disordered tetrahedra, T(1D) and T(2D). The T(1D)-T(2D) separation of 1.3 Å requires an ordering scheme between the disordered tetrahedral sites. In addition, M suggests 0.5B + 0.2Si at the T(1D) site. Ordering schemes for only one species, say T(1D), can be admitted for full occupancy by *I4/mmm* or *I*422. For both ordered and fully occupied T(1D) and T(2D), *I4mm, I*$\bar{4}$*2m, Immm,* and their subgroups are possibilities. To test these subgroups was considered but deemed of marginal value, owing to high parameter correlations and, in most cases, a near-doubling of variable atomic coordinate parameters. Therefore, we proceeded in *I4/mmm,* realizing that an averaged crystal structure would result. Incidentally, such an averaged structure may well explain a few anomalies (such as nonpositive definite thermal ellipsoids) in the refinements.

Table 4 lists the thermal parameters, Table 5[1] the structure factors, and Table 6 the bond distances and angles. These tables report results of both the MSS and M studies, and all but Table 5 are grouped together for easy comparison. Mention should be made of refinement procedures. In both MSS and M, the atomic coordinate parameters and anisotropic thermal parameters were refined for the "healthy" part, and all atoms fully occupied their sites. For the "pathological" part of the structure, parameter

[1] To obtain a copy of Table 5, order Document AM-87-360 from the Business Office, Mineralogical Society of America, 1625 I Street, N.W., Suite 414, Washington, D.C. 20006, U.S.A. Please remit $5.00 in advance for the microfiche.

TABLE 4. Ashcroftine: Anisotropic thermal-vibration parameters ($\times 10^4$)

Atom	U_{11}	U_{22}	U_{33}	U_{23}	U_{13}	U_{12}		Atom	U_{11}	U_{22}	U_{33}	U_{23}	U_{13}	U_{12}	
			(Healthy section)								(Healthy section, continued)				
Si(1)	229(19)	96(17)	80(16)	−31(14)	−9(15)	26(15)		OH(1)	83(49)	83	5(75)	0	0	18(66)	
	175(14)	134(14)	109(12)	−16(11)	4(11)	36(11)			147(45)	147	267(83)	0	0	75(58)	
Si(2)	377(24)	84(17)	101(18)	−19(15)	60(17)	−28(18)		OW(1)	904(102)	904	328(89)	−417(84)	−417	697(123)	
	284(17)	99(13)	152(14)	−20(11)	66(12)	−45(12)			386(48)	386	157(50)	−228(42)	−228	263(60)	
Si(3)	320(21)	97(17)	133(18)	5(15)	1(16)	−13(16)		OW(2)	345(184)	380(190)	178(152)	0	0	0	
	230(16)	119(14)	223(16)	7(12)	−41(13)	−3(12)			304(157)	610(209)	189(124)	0	0	0	
O(1)	467(61)	207(49)	100(44)	−132(43)	124(48)	−10(45)	NPD	Y(1)	167(6)	277(7)	113(5)	35(6)	0(6)	52(6)	
	231(39)	163(36)	223(38)	−35(34)	60(36)	−41(31)			129(5)	194(6)	125(4)	29(5)	−9(4)	31(4)	
O(2)	408(61)	275(52)	102(46)	−17(42)	19(44)	−61(51)		Y(2)	181(10)	149(10)	114(9)	0	0	3(8)	
	362(52)	245(45)	228(41)	−58(36)	18(39)	−32(40)			151(9)	127(9)	110(8)	0	0	5(6)	
O(3)	172(49)	199(49)	246(48)	−74(42)	2(42)	79(40)		K(1)	493(54)	854(72)	428(49)	0	0	0	
	179(38)	211(39)	258(40)	−34(35)	15(34)	17(31)			573(48)	364(38)	490(42)	0	0	0	
O(4)	266(51)	184(47)	202(51)	49(43)	−14(43)	12(42)		K(2)	662(65)	669(64)	411(50)	0	0	0	
	288(45)	217(41)	253(43)	50(37)	14(38)	9(35)			505(46)	605(51)	376(37)	0	0	0	
O(5)	256(51)	190(49)	173(48)	−24(40)	84(41)	−50(41)		Na(1)	258(59)	258	679(135)	0	0	0	
	213(41)	194(39)	257(42)	−35(33)	77(34)	−25(32)			206(44)	206	593(107)	0	0	0	
O(6)	212(58)	519(74)	882(95)	296(74)	−76(64)	70(55)									
	249(53)	491(70)	1210(116)	331(77)	−83(67)	−54(49)					(Pathological section)				
O(7)	192(42)	192	21(52)	−62(39)	−62	135(55)	NPD	T(1D)	37(49)	37	13(76)	146(47)	146	2(65)	NPD
	135(31)	135	212(50)	−29(32)	−29	53(41)					223(28)				
O(8)	485(93)	123(68)	56(59)	0	0	−78(65)		T(2D)	134(61)	134	71(92)	−32(55)	−32	−74(82)	
	352(69)	155(57)	153(51)	0	0	−48(49)					258(57)				
O(9)	490(98)	86(65)	201(71)	0	39(72)	0		K(1D)	1510(205)	1510	963(229)	−14(144)	−14	−665(267)	
	439(80)	154(56)	232(58)	0	55(60)	0			930(142)	930	897(209)	−116(124)	−116	−279(184)	
O(10)	884(126)	49(63)	154(70)	0	−21(80)	0		Na(1D)	295(133)	236(109)	558(156)	0	69(113)	0	
	883(123)	202(64)	235(65)	0	−120(76)	0			404(121)	527(134)	905(183)	0	191(132)	0	
C(1)	246(129)	660(180)	428(155)	0	−40(124)	0		Na(2D)	496(244)	1(127)	618(256)	0	201(220)	0	
	329(104)	521(129)	262(97)	0	−23(86)	0			571(134)	148(76)	1366(255)	0	−629(168)	0	
O(11)	446(71)	435(69)	627(81)	3(67)	24(66)	4(59)		Na(3D)	−313(87)	−313	7257(1422)	0	0	0	NPD
	414(57)	293(51)	630(69)	5(53)	11(56)	−4(44)					266(97)				
O(12)	288(97)	1579(216)	423(113)	0	−135(92)	0		ϕ(1D)	286(111)	286	663(224)	307(127)	307	−49(149)	NPD
	235(78)	1202(167)	590(113)	0	−54(83)	0					312(73)				
C(2)	499(168)	597(189)	219(137)	0	0	217(157)	NPD	ϕ(2D)	344(174)	344	353(277)	54(131)	54	−506(213)	NPD
	273(95)	233(91)	273(85)	0	0	34(73)					770(227)				
O(13)	501(69)	282(57)	148(49)	−36(46)	−53(52)	83(53)		ϕ(3D)	1(451)	167(587)	1(427)	0	0	−47(432)	NPD
	468(58)	245(45)	180(38)	−4(35)	29(41)	35(42)					790(292)				
O(14)	356(88)	229(83)	245(71)	0	0	−101(73)		ϕ(4D)	496(176)	496	1(169)	0	0	−280(230)	
	303(69)	184(59)	236(55)	0	0	−44(52)					623(182)				
								ϕ(5D)	429(450)	22(270)	1354(668)	0	0	0	
											1313(334)				
								ϕ(6D)	222(191)	222	1546(719)	0	0	48(221)	
											1105(383)				

Note: For each pair, the first row is from MSS, the second row from M. NPD means nonpositive definite ellipsoid. In the pathological section, most of M are isotropic thermal refinements, the MSS values often nonpositive definite. The entries are coefficients in the expression $\exp -[U_{11}h^2 + U_{22}k^2 + U_{33}l^2 + 2U_{23}kl + 2U_{13}hl + 2U_{12}hk]$. Estimated standard errors refer to the last digit except for those coefficients related by symmetry.

correlations among site occupancies, scattering curves, and thermal vibration ellipsoids are high. Refinement varying all such parameters rarely has much meaning. MSS approximately refined occupancy parameters, then fixed them while continuing anisotropic thermal refinement. M allowed occupancies to vary but continued with isotropic refinement.

By adding up the cell contents from the refined crystal structure, an approximate formula for ashcroftine can be computed, as presented in Table 1 and Table 2. The minor MgO, MnO, and substantial CaO (5.72%) were ignored, and all OW (= H_2O) and CO_2 determined from the structure study were included in the oxide content calculated from the formula. Note that all Al_2O_3 of Gordon (1924) was reckoned as Y_2O_3. Clearly, more (H_2O) occurs in the structure, but this is probably disordered—hence undetected by X-ray diffraction—in the large ball. Although the alkali contents are in fair agreement, Whitfield's analysis suggests that CaO indeed goes into solution with Y_2O_3.

Oddly, the calculated density based on the proposed formula stands in surprisingly good agreement with the specific gravity determinations of Hey and Bannister (1933). This agreement is probably fortuitous and is in part the cumulation of many small errors (neglect of CaO, uncertain H_2O in cell, other absences, possible incorrect atom assignments). For this reason, calculated specific gravities of complex minerals, so often used to confirm a formula in the literature, can be delusive.

Description of the structure

The elephantine crystal structure of ashcroftine has regions or subunits that possess very high point symmetry, $4/m\ 2/m\ 2/m$ and its subgroups. We are particularly concerned about specific regions in the structure—in this case, three—that warrant individual description and conclude with a unified description of the entire structure.

The first region consists of the ordered silicate and carbonate fractions of the structure in the unit cell, specifically $[Si_{48}O_{128}]$ and $16[CO_3]$ for $Z = 2$. These two radicals include the first 19 nonequivalent atomic sites in Table 3, all of them ordered and fully occupying their positions. We call this stable region of the structure the *curd.* Mandelbrot (1983, p. 76), who introduced this neologism, defined it as "a volume within which a physical characteristic becomes increasingly concentrated as a result of curdling." On that same page, he defines *curdling* as "any cascade of instabilities resulting in a contraction." In other words, a curd is the limit of a converging set. This definition, although it is used in the description of fractal geometries, appears quite appropriate in describing crystal structures—in this case, the region that is ordered and that itself conserves the point symmetry of the space group. We shall also call this region, specifically $[Si_{48}O_{128}]$, the *fundamental building block* of the crystal structure.

The second region follows from the first and is also defined by Mandelbrot (1983, p. 76). It is the *whey* or "the space outside the curd." This term is appropriate as it includes the extensively disordered part composed of 12 nonequivalent atomic sites and as we could not find any stable (ordered and fully occupied) sites *within* the domain of the whey.

The third region is a portion of the curd and the whey. Specifically, it is the region that is adjacent to the curd and to the whey. An appropriate term is *limbus.* Consulting Bethel (1956, p. 488), limbus is of Latin etymology and specifically applies to zoology and botany—"a border distinguished by color or structure." It is proposed that limbus also applies to chemical crystallography. It is where the curd overlaps with the whey. The limbus includes the terminal oxyanions from the curd that also coordinate to the adjacent cations: Y(1), Y(2), Na(1), Na(2D), K(1), K(2), and Na(1D).

The curd

The curd is centered at (0 0 ½), (½ ½ 0) for the silicate fraction; and (½ 0 ¼), (½ 0 ¾), (0 ½ ¾), and (0 ½ ¼)—which exactly specify the centroids of Na(1)—for the carbonate fraction. It includes Si(1) to Si(3), O(1) to O(10); Na(1); C(1), O(11), O(12); and C(2), O(13), O(14). The stoichiometry in the cell is $2[Si_{48}O_{128}]$ and $[Na(1)_4(CO_3)_{32}]$. All 20 nonequivalent atoms are ordered and their sites fully populated (Table 3). The curd is shown in Figure 1 as a spoke diagram.

The ordered silicate fraction is most interesting. Its dimensionality is 0, and it is therefore either an oligosilicate unit, the largest yet found in a mineral crystal, or a cyclosilicate. Its composition is $[Si_{48}O_{128}]$, which rules out monocyclosilicates, where $[Si_pO_{3p}]$ obtains. This is an adequate but incomplete description of the silicate unit in ashcroftine. In a remarkable but rarely cited paper by Laves (1932) on silicate classification, particular emphasis is placed on *dimensionality.* For dimensionality = *n,* he derived for stoichiometry of tetrahedral units SiO_4, $n = 0$; SiO_3, $n = 0, 1$; Si_2O_5, $n = 0, 1, 2, 3$; and SiO_2, $n = 1, 2, 3$ as topological possibilities. The stoichiometry for ashcroftine is $16Si_3O_8$. It can be mapped on the surface of a ball, that is, it conserves a *volume,* by merely connecting the Si cations together (a connection whenever a linking oxygen exists). Such arrangements we prefer to consider a subdivision of the oligosilicates, and we call them *balosilicates,* from Middle English *bal* meaning "ball."

One important property of the balosilicate is that the oligosilicate anionic unit maps on a sphere and it possesses branches (connections or edges), vertices (nodes), and polygons (faces) that together can refer to some polyhedron. Such systems must have some connections greater than two about vertices. Two-connected systems (such as rings) merely divide the sphere into two pieces by the intervening polygon. Liebau (1985) in a masterful discussion on silicate structures, listed the dicyclosilicate double rings. With p = number of tetrahedra within one ring, the general formula is $[^pSi_{2p}O_{5p}]^{-2p}$. Double rings are known for $p = 3$ (synthetic phases), 4 (numerous synthetic phases, steacyite, iraqite), 5 (synthetic phases), and 6 (synthetic phases, minerals of the osumilite-milarite group). It is proposed that all double-ring silicates whose connections of vertices define a polyhedron also be called *balosilicates.*

Connecting the cations together in Figure 2 gives the $[Si_{48}]$ ball. Here, nodes identify with the Si cations and

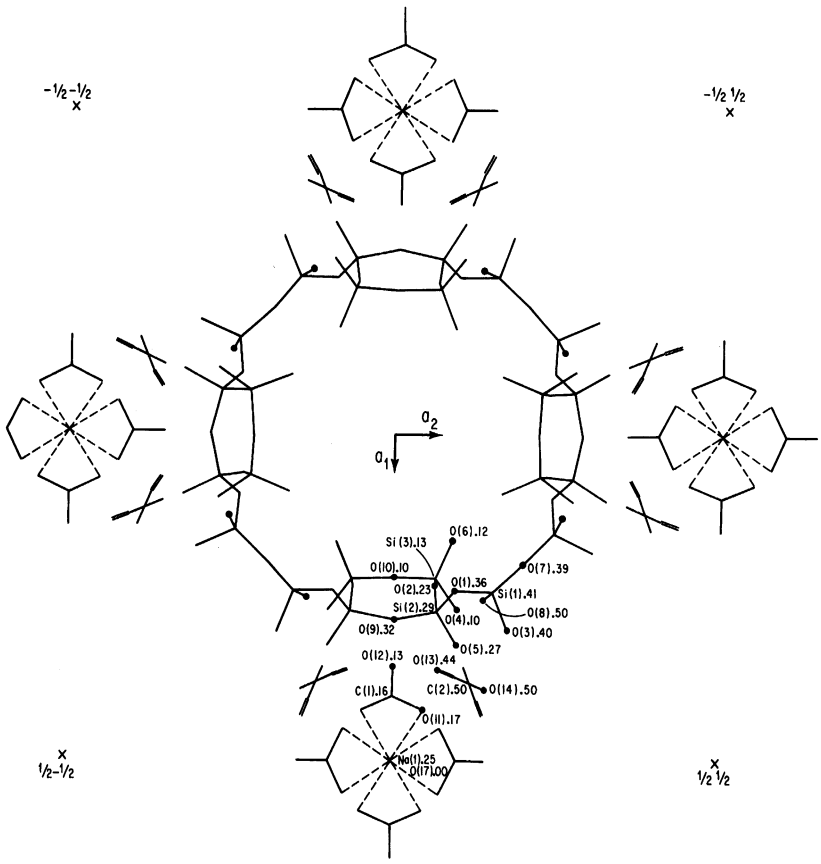

Fig. 1. The central curd of ashcroftine as a spoke diagram, showing Si(1) to Si(3), C(1), C(2), Na(1), O(17) = OW(2) and O(1) to O(14). These atoms are ordered. The ball centered at (0 0 ½) is $[Si_{48}O_{128}]$. Atom sites corresponding to Table 3 are noted, and their heights are given as fractional coordinates in z.

edges with the connecting oxide anions where the oxides occur somewhere near the midpoints of these edges. Eight cuts occur above and below the plane of the projection and are represented diagrammatically as dashed lines. For each dashed line, not one oxide occurs, but two. If these eight oxide pairs are fused together, then the stoichiometry is $[Si_{48}O_{120}]$. This leads to Figure 3, which is the plan of the truncated cuboctahedron, an Archimedean semiregular solid.

Figure 4 attempts to feature a combination of polyhedral and spoke representations of the crystal structure, the central $[Si_{48}O_{128}]$ unit and its enveloping limbus of Y(1)–O, Y(2)–O, K(1)–O, K(2)–O, Na(2D)–O, and Na(3D)–O bonds (the last two atom positions in the whey). Also in the whey are T(1D), which is shown here, and T(2D) that seal the dashed ruptures in Figure 2 together. Through additional units such as $[T(D)_2\phi(D)\phi(D)_2O_4]$ or $[T_2O_7]$ groups, the balls are bridged together along [001]. For this reason, the tetrahedral fraction can be considered tubular with enormous bulges in it. The tubular portion then is $^1_\infty[T_{56}O_{140}]$, T connoting tetrahedrally coordinated cations such as Si^{4+} or B^{3+}. Note that in the process, semiregularity is destroyed for the ideal truncated cuboctahedron (t.c.o.). Instead, from $N_0 = 48$, $N_1 = 72$, and $N_2 = 26$ (12 squares, 8 hexagons, 6 octagons), insertion of disordered T(D) tetrahedra lead to $N_0 = 56$, $N_1 = 80$, $N_2 = 26$ (12 squares, 4 octagons, 8 heptagons, 2 dodecagons). We shall see later that this insertion leads to a geometrical as well as point-symmetric distortion of the t.c.o. The $(4/m\ \bar{3}\ 2/m)$ point symmetry of the t.c.o. is degraded to a nearest subsymmetry $(4/m\ 2/m\ 2/m)$. This is also the average point symmetry of ashcroftine's crystal structure.

Two independent carbonate groups and Na(1) complete the curd. The $[Na(1)O_8]$ polyhedron serves in part as a bridge between the $[Y(1)O_8]$ polyhedra along [100] and [010]. Four $[C(1)O(12)O(11)_2]$ polyhedra surround the central Na(1) that is fixed on the tetragonal scalenohedral point $(\bar{4}m2)$. Four O(11)-O(11)′ edges are identified with edges of the $[Na(1)O(11)_8]$ polyhedron that is a cube (polyhedron no. 257 of Britton and Dunitz, 1973), distorted by unequal edge lengths toward the direction of a square antiprism (polyhedron no. 128). These linkages and the $[C(2)O(14)O(13)_2]$ polyhedron show up as islands in Figure 1, the latter appearing like crossed swords. The oxygen atoms in this latter $[C(2)O_3]$ group are also linked with Y(1) through edge-sharing via O(13)-O(14). The for-

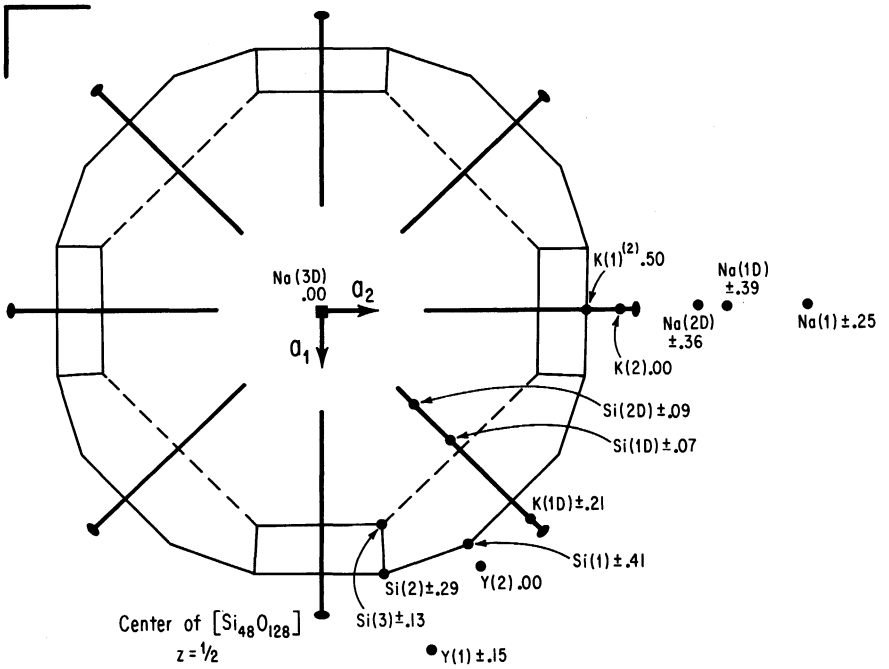

Fig. 2. The central ball drawn as $[Si_{48}]$ connections, with mirror planes and twofold and fourfold rotors drawn in. The linking oxygen atoms are approximately at the midpoints of the "edges." The breaks of the edges for the truncated cuboctahedron are shown as dashed lines. There are eight such dashed lines, each representing two oxygens instead of one such that $Si_{48}O_{120} + O_8 = Si_{48}O_{128}$. Surrounding cations in the border or limbus and cations in the disordered whey are also shown, heights as fractional coordinates in z following Table 3.

mer $[C(1)O_3]$ group also shares an O(11)-O(12) edge with Y(1). As the $[CO_3]$ groups are constrained by mirror planes, they act as structural struts, and $[C(1)O_3]$ bridges by two O(11)-O(12) edges to Y(1) along [100] (and [010]); $[C(2)O_3]$ bridges by two O(13)-O(14) edges to Y(1) along [001].

The limbus

The border or edge between the ordered curd and the disordered whey includes the remaining ordered cations Y(1), Y(2), K(1), and K(2). They define a laurel wreath around the central $[Si_{48}O_{128}]$ curd, and the chicken-egg question arises: just which portion of the total structure was the template for the remainder? A possible answer can be found in assessing the point symmetries. The central laurel wreath has overall composition $8Y_6^{3+}O_{28}\phi(D)_2OH$, which includes one of the disorderd anions. It involves a sequence of Y(1)-Y(2)-Y(2)-Y(1) face-sharing polyhedra (Fig. 5). The polyhedra are now discussed. The $[Y(1)O_8]$ polyhedron is ideally a *D2d* dodecahedron (polyhedron no. 14), a common coordination polyhedron of order eight about lanthanides. For example, in cerite, $Ce_9Fe^{3+}(SiO_4)_6(SiO_3OH)(OH)_3$, all three nonequivalent lanthanide positions are based on the *D2d* dodecahedron. The $[Y(2)O_8]$ polyhedron is more elusive since it includes disordered ϕ(1D), but if full occupancy of this anion is granted, the polyhedron is also of order eight. With Y(2) at $z = 0$, coordinating O(3), O(4), and ϕ(1D) with general z define a distorted trigonal prism; two coordinating atoms at $z = 0$, OH(1), and O(14) form the two lateral caps and complete the polyhedron that is a bicapped trigonal prism (polyhedron no. 52). The max-

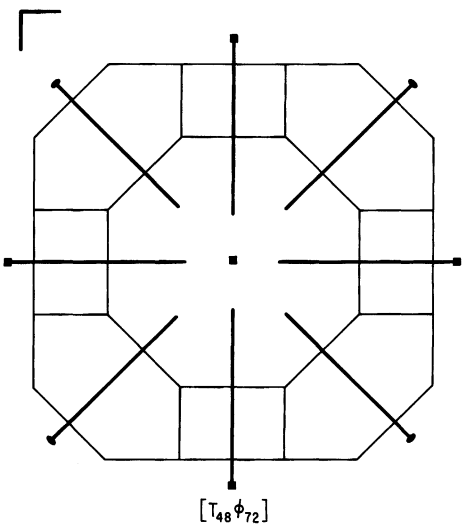

Fig. 3. The Archimedean semiregular truncated cuboctahedron down an axis normal to the octagonal face. Mirror planes and twofold and fourfold rotors are drawn in. The polyhedron has $N_0 = 48$ vertices and $N_1 = 72$ edges.

TABLE 6. Ashcroftine bond distances (Å) and angles (°)

(Healthy part)

Si(1)				
Si(1)–O(3)	1.595(9)		1.590(8)*	
Si(1)–O(8)	1.617(6)		1.628(5)*	
Si(1)–O(7)	1.619(10)		1.631(8)*	
Si(1)–O(1)	1.622(9)		1.624(8)*	
Average	1.613		1.618*	
O(1)–O(8)	2.56(1)	104.2(6)	2.57(1)*	104.3(5)*
O(1)–O(7)	2.62(1)	107.6(5)	2.59(1)*	105.5(4)*
O(7)–O(8)	2.63(1)	108.8(7)	2.64(1)*	108.5(6)*
O(1)–O(3)	2.64(1)	110.4(5)	2.64(1)*	110.6(4)*
O(3)–O(8)	2.66(1)	111.6(6)	2.68(1)*	112.9(6)*
O(3)–O(7)	2.69(1)	113.7(5)	2.71(1)*	114.3(4)*
Average	2.63	109.4	2.64*	109.4*
Si(2)				
Si(2)–O(5)	1.591(10)		1.597(8)*	
Si(2)–O(9)	1.611(6)		1.629(5)*	
Si(2)–O(1)	1.622(10)		1.626(9)*	
Si(2)–O(2)	1.629(10)		1.614(10)*	
Average	1.613		1.616*	
O(1)–O(2)	2.55(1)	103.6(5)	2.55(1)*	104.0(5)*
O(1)–O(9)	2.59(1)	106.6(6)	2.61(1)*	106.6(5)*
O(2)–O(9)	2.61(1)	107.3(6)	2.63(1)*	108.2(6)*
O(2)–O(5)	2.67(1)	112.0(5)	2.66(1)*	112.1(5)*
O(1)–O(5)	2.68(1)	113.0(5)	2.69(1)*	113.0(4)*
O(5)–O(9)	2.68(1)	113.8(7)	2.68(1)*	112.4(6)*
Average	2.63	109.4	2.64*	109.4*
Si(3)				
Si(3)–O(6)	1.571(11)		1.589(10)*	
Si(3)–O(4)	1.586(10)		1.588(10)*	
Si(3)–O(10)	1.603(6)		1.619(6)*	
Si(3)–O(2)	1.624(9)		1.617(9)*	
Average	1.596		1.603*	
O(2)–O(6)	2.54(1)	105.5(6)	2.57(2)*	106.8(7)*
O(6)–O(10)	2.56(1)	107.6(8)	2.58(2)*	107.0(8)*
O(4)–O(10)	2.60(1)	109.3(7)	2.60(1)*	108.3(7)*
O(2)–O(10)	2.62(1)	108.5(6)	2.65(1)*	109.6(6)*
O(4)–O(6)	2.64(1)	113.6(6)	2.66(1)*	113.5(6)*
O(2)–O(4)	2.66(1)	112.0(5)	2.65(1)*	111.4(5)*
Average	2.60	109.4	2.62	109.4

C(1)				
1 C(1)–O(12)	1.23(2)		1.30(3)*	
2 C(1)–O(11)	1.30(3)		1.29(1)*	
Average	1.28		1.29*	
2 O(11)–O(12)	2.20(2)	120.5(10)	2.23(2)*	119.0(9)*
1 O(11)–O(11)^{A}	2.25(2)	119.1(19)	2.25(1)*	122.0(16)*
Average	2.22	120.0	2.24*	120.0*
C(2)				
2 C(2)–O(13)	1.29(1)		1.28(1)*	
1 C(2)–O(14)	1.29(3)		1.28(2)*	
Average	1.29		1.28*	
2 O(13)–O(14)	2.21(2)	118.4(10)	2.21(1)*	119.2(9)*
1 O(13)–O(13)^{B}	2.27(1)	123.2(20)	2.24(1)*	121.6(16)*
Average	2.23	120.0	2.22*	120.0*
Y(1)				
Y(1)–O(5)^{C}	2.321(8)		2.333(9)*	
Y(1)–O(3)^{C}	2.321(8)		2.341(7)*	
Y(1)–O(4)	2.322(9)		2.330(10)*	
Y(1)–O(5)	2.363(9)		2.370(8)*	
Y(1)–O(13)^{C}	2.382(10)		2.407(9)*	
Y(1)–O(11)	2.395(11)		2.398(10)*	
Y(1)–O(14)^{C}	2.580(2)		2.580(2)*	
Y(1)–O(12)	2.779(2)		2.766(2)*	
Average	2.433		2.441*	
Y(1)–C(2)^{E}	2.88(1)		2.88(1)*	
Y(2)				
1 Y(2)–OH(1)^{C}	2.21(1)		2.22(1)*	
2 Y(2)–O(4)	2.29(1)		2.29(1)*	
1 Y(2)–ϕ(6D)	2.29(4)		2.20(6)*	
2 Y(2)–O(3)^{C}	2.30(1)		2.32(1)*	
2 Y(2)–ϕ(1D)	2.46(3)		2.47(2)*	
1 Y(2)–O(14)^{C}	2.55(2)		2.60(1)*	
Average	2.35		2.35*	

K(1)		
4 K(1)–O(13)	2.94(1)	2.93(1)*
2 K(1)–O(9)	3.15(1)	3.14(1)*
2 K(1)–O(8)	3.32(1)	3.32(1)*
4 K(1)–O(1)	3.36(1)	3.39(1)*
Average	3.18	3.18*
2 K(1)–C(2)	3.27(3)	3.29(3)*
K(2)		
2 K(2)–O(12)	2.57(2)	2.57(2)*
2 K(2)–O(10)	2.74(2)	2.74(2)*
2 K(2)–O(14)^{C}	2.86(2)	2.86(1)*
4 K(2)–O(4)	3.01(1)	2.98(1)*
Average	2.84	2.83*
4 K(2)–Si(3)	3.48(1)	3.49(1)*
Na(1)		
8 Na(1)–O(11)	2.51(1)	2.51(1)*
Si–O–Si′ angles		
Si(1)–O(1)–Si(2)	137.9(7)	138.1(5)*
Si(1)–O(7)–Si(1)^{D}	142.5(7)	141.0(7)*
Si(1)–O(8)–Si(1)^{B}	141.7(9)	140.4(8)*
Si(2)–O(2)–Si(3)	141.1(7)	143.1(7)*
Si(2)–O(9)–Si(2)^{A}	141.8(9)	140.1(9)*
[Si(2)–O(1)–Si(1)	137.9(7)	138.1(5)*]
Si(3)–O(10)–Si(3)^{A}	140.8(9)	139.0(9)*
[Si(3)–O(2)–Si(2)	141.1(7)	143.1(7)*]
Si(3)–O(6)–T(1D)	138.5(9)	138.5(9)*
Si(3)–O(6)–T(2D)	167.2(10)	165.9(10)*

Note: Estimated standard errors refer to the last digit. The equivalent positions (referred to Table 3) are designated as superscripts and are (*A*) $x, -y, z$; (*B*) $x, y, -z$; (*C*) $\frac{1}{2} - y, \frac{1}{2} - x, \frac{1}{2} - z$; (*D*) y, x, z; (*E*) $\frac{1}{2} - y, \frac{1}{2} - x, \frac{1}{2} + z$.

* Results of Merlino. Other results are those of Moore, Sen Gupta, and Schlemper.

TABLE 6. *Continued*

					(Pathological part)
		T(1D) [2 O(6), 1 ϕ(1D), 1 ϕ(4D)]			
2 T(1D)–O(6)		1.54(2)		1.51(2)*	
1 T(1D)–ϕ(4D)		1.67(2)		1.79(3)*	
1 T(1D)–ϕ(1D)		1.79(2)		1.67(2)*	
Average		1.64		1.62*	
2 T(1D)–ϕ(3D)		1.33(5)		1.31(3)*	
1 T(1D)–ϕ(6D)		1.78(3)		1.89(5)*	
1 O(6)–O(6)^D	2.44(2)	105.0(11)	2.40(2)*	105.5(12)*	
2 ϕ(4D)–O(6)	2.52(2)	103.5(12)	2.55(3)*	100.8(13)*	
2 ϕ(1D)–O(6)	2.54(3)	99.2(12)	2.46(2)*	101.4(10)*	
1 ϕ(1D)–ϕ(4D)	3.26(5)	142.2(16)	3.29(4)*	142.9(14)*	
Average	2.64	108.8	2.62*	108.8*	
		T(1D) [2 O(6), 1 ϕ(4D), 1 ϕ(6D)]			
1 O(6)–O(6)^D	2.44(2)	105.0(11)	2.40(2)*	105.5(12)*	
2 ϕ(4D)–O(6)	2.52(2)	103.5(12)	2.55(3)*	100.8(13)*	
1 ϕ(4D)–O(6D)	2.53(5)	94.8(13)	2.81(7)*	99.8(15)*	
2 ϕ(6D)–O(6)	2.91(3)	122.5(14)	2.98(4)*	122.3(19)*	
Average	2.64	108.6	2.71	108.6	
		T(2D)			
2 T(2D)–O(6)		1.55(2)		1.54(2)*	
1 T(2D)–ϕ(4D)		1.58(2)		1.58(2)*	
1 T(2D)–ϕ(2D)		1.67(3)		1.61(6)*	
Average		1.59		1.57*	
1 O(6)–O(6)^D	2.44(2)	104.0(10)	2.40(2)*	102.5(10)*	
2 O(6)–ϕ(4D)	2.52(2)	107.0(15)	2.55(3)*	109.4(17)*	
2 O(6)–ϕ(2D)	2.69(3)	113.1(15)	2.65(5)*	114.4(23)*	
1 ϕ(2D)–ϕ(4D)	2.70(4)	112.2(20)	2.57(7)*	106.8(30)*	
Average	2.59	109.4	2.56	109.5	
T–ϕ–T′ angles					
T(2D)–ϕ(4D)–T(2D)		179.7(22)		170.6(27)*	
T(1D)–ϕ(3D)–T(1D)		120.3(75)		129.0(57)*	
T(1D)–ϕ(4D)–T(2D)		134.6(18)		126.6(21)*	
T(1D)–ϕ(4D)–T(1D)		88.8(15)		82.6(16)*	
T(1D)–ϕ(6D)–T(1D)		81.5(17)		77.7(23)*	

	K(1D)	
1 K(1D)–ϕ(1D)	2.47(5)	2.58(4)*
1 K(1D)–O(7)	3.24(4)	3.18(4)*
1 K(1D)–OW(1)	3.29(4)	3.17(3)*
2 K(1D)–O(3)^C	3.21(4)	3.25(3)*
Average	3.08	3.09*
1 K(1D)–K(1D)^C	2.79(4)	2.81(4)*
	Na(1D)	
2 Na(1D)–O(11)	2.26(2)	2.22(2)*
2 Na(1D)–O(13)	2.30(2)	2.34(2)*
1 Na(1D)–OW(2)	2.74(2)	2.65(3)*
Average	2.37	2.35*
1 Na(1D)–Na(2D)	0.90(3)	0.94(1)*
	Na(2D)	
2 Na(2D)–O(13)	2.26(4)	2.24(2)*
2 Na(2D)–O(11)	2.39(3)	2.38(2)*
1 Na(2D)–O(9)	2.67(4)	2.71(3)*
Average	2.39	2.39*
	Na(3D)	
Na(3D)–ϕ(5D)	2.49(1)[×4]**	2.70(7)[×4]*
Na(3D)–ϕ(2D)	2.86(1)[×8]**	2.45(7)[×4]*
Average	2.74**	2.58*
Na(3D)–ϕ(4D)	3.33(8)[×4]**	3.27(4)[×4]*
Na(3D)–ϕ(2D)^B	—	3.30(7)[×4]*

** Na(3D) fixed at (0 0 0).

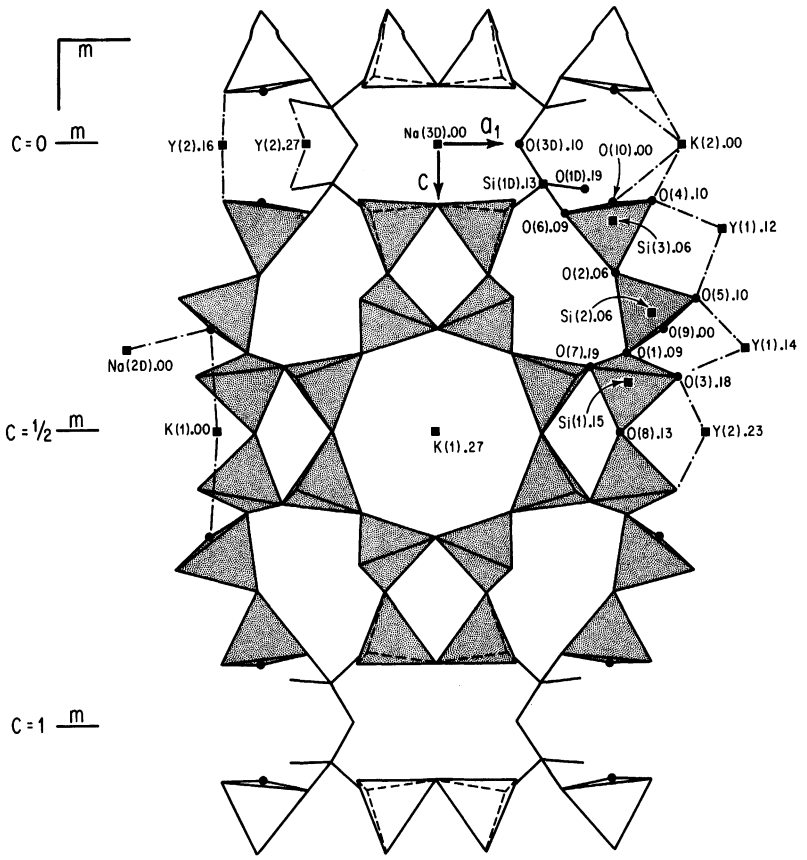

Fig. 4. Ashcroftine's central $[Si_{48}O_{128}]$ ball drawn as stippled polyhedra projected down [010]. Some cations in the limbus and whey are shown. At least five different $[T_2O_7]$ bridges between the neighboring balls can occur along [001]. One of them—Si(1D)–O(3D)–Si(1D) [= T(1D)–ϕ(4D)–T(1D) in text]—is shown. Heights are given as fractional coordinates in y. Note that the top and bottom portions of adjacent balls along [001] are drawn in as unshaded polyhedra.

imal point symmetries for $Y(1)O_8$ and $Y(2)O_8$ are $D2d$ = ($\bar{4}2m$) and $C2v$ = ($mm2$) respectively. The twelve-coordinated K(1) cation is situated near the center of and just outside the large octagonal windows of the central curd (Figs. 2, 4, and 5) and occurs within a distorted $[K(1)O(8)_2O(9)_2O(1)_4O(13)_4]$ tetracapped square prism, the O(8) and O(9) defining the caps. The polyhedron has maximal point symmetry $C2v$ = ($mm2$). The K(2) cation is ten-coordinated with composition $[K(2)O(10)_2O(12)_2O(14)_2O(4)_4]$ and also appears in Figures 2, 4, and 5. This cation is further removed from the central curd, more situated in the direction of the interceding channels. It is a distorted *cis*-bicapped square prism, the two O(14) caps in the plane of central K(2). The maximal point symmetry is also ($mm2$). For larger cations, it is often difficult to decide which are the nearest-neighbor distances. Therefore, in Table 6, which lists bond distances, the first cation-cation distance is also listed separately.

This completes description of the curd and limbic portions of the ashcroftine crystal structure that contain 27 independent atoms out of at least 39 independent atoms in the crystal structure. It is believed that the point symmetry $D4h$ = ($4/m$ $2/m$ $2/m$) for the ordered fragment of the $[Si_{48}O_{128}]$ ball suggests that it is indeed a fundamental building block (f.b.b.). In fact, the two distinct $Y\phi_8$ polyhedra possess neither symmetry nor any simple explanation for their structural design other than that $[Si_{48}O_{128}]$ forced their arrangement and with them, the arrangements of all the other atoms in the limbus and in the whey. It is suggested that in the chicken-egg paradox, the egg came first and was the balosilicate fraction.

The whey

In the whey, the tetrahedrally coordinated cations are symbolized by T and the ligands by ϕ. All atoms are suffixed by D to indicate their disordered nature. The disordered portion of the crystal structure is composed of at least twelve nonequivalent "pathological" atoms (Table 3). This portion of the study constituted by far the most tedious and frustrating part. Since MSS and M worked on the structure largely independently, it is gratifying that at least approximate convergence was attained for the disordered atoms even though the methods for their deciphering and refinement were somewhat different.

Nomenclature for the six disordered cations includes

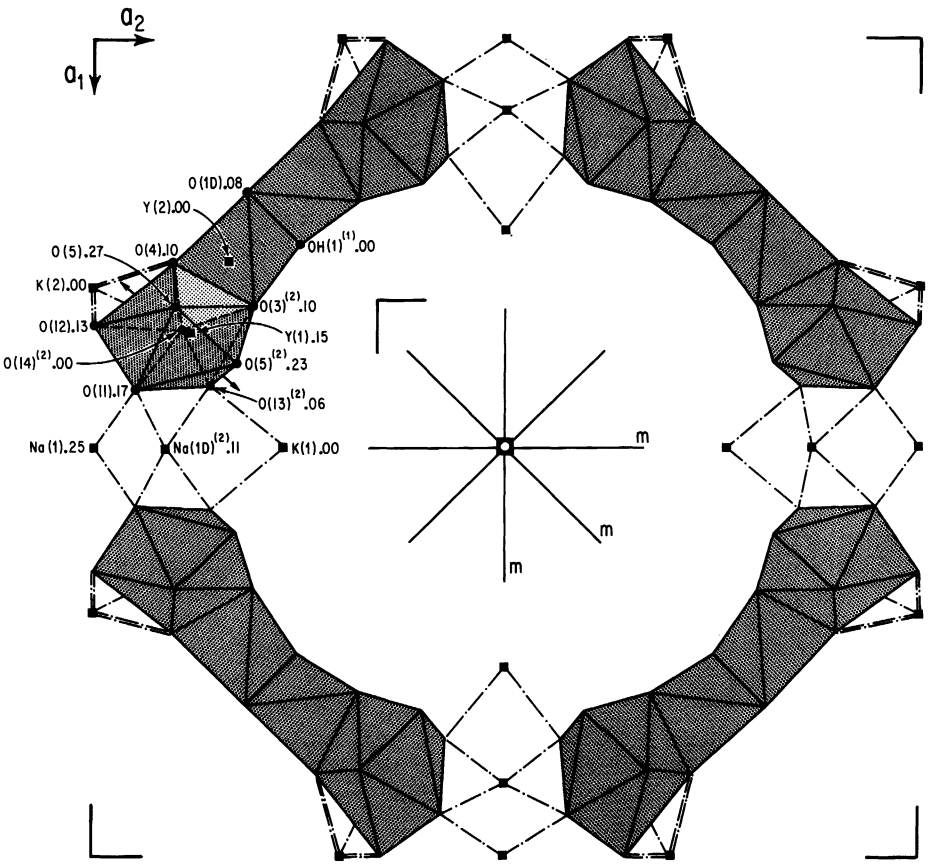

Fig. 5. The limbus in ashcroftine that encrusts the central curd. The Y(1)-O and Y(2)-O polyhedra are stippled. Some Na(1)–O, Na(1D)–O, K(1)–O and K(2)–O bonds are shown. The laurel wreath shown here is centered at (½ ½ 0), and some elements of symmetry are shown. Heights are given in fractional coordinates in z.

T(1D) and T(2D) for tetrahedrally coordinated small cations and K(1D), Na(1D), Na(2D), and Na(3D) for larger cations; ϕ(1D) to ϕ(6D) designate the disordered coordinating ligands (O^{2-}, OH^-, H_2O). K(1D) is close to the inversion center at (¼ ¼ ¼) with K(1D)-K(1D)′ ≈ 2.8 Å and therefore occupies at most half its site. Na(1D) and Na(2D) with Na(1D)-Na(2D) ≈ 0.9 Å occur in a complementary relation with each other. M proposes half-occupancy at each site, whereas MSS suggest a more asymmetrical distribution. Na(3D) is in a fixed position at (0 0 0) in MSS (note severe thermal anisotropy in Table 4), whereas M chose (0 0 z), the distance between the two centroids being 0.56 Å. In the first case Na(3D) is in a twelve-coordinate site, with four ϕ(5D) and eight ϕ(2D) at vertices; in the latter case Na(3D) is in an eight-coordinate site, with four ϕ(5D) and four ϕ(2D) at vertices. A complementary relation exists between two disordered anions, ϕ(1D) and ϕ(6D). These evidently coordinate to Y(2). But ϕ(1D)-ϕ(6D) ≈ 1.4 Å requires occupancies for adjacent pairs ϕ(1D) = 0.0, ϕ(6D) = 1.0 or ϕ(1D) = 1.0, ϕ(6D) = 0.0 or coordination numbers for Y(2) of seven and eight, respectively.

At least five spanners or bridges can be identified between $[Si_{48}O_{128}]$ balls along [001]. One of these—T(1D)–ϕ(4D)–T(1D)—is shown as a spoke diagram in Figure 4 and is one of the unlikely ones. From O(6)-O(6)[2] related by the mirror plane at z = 0, the distance along [001] is ≈4.0 Å, roughly the gap spanned by a $[T_2O'O_6]$ oligosilicate dimer where O′ is shared by two T. For the ball centered at (0 0 ½), the tetrahedral centers are T = T(1D), T(2D), and the geometrically permissible O′ links are O′ = ϕ(3D), ϕ(4D), and ϕ(6D). The possible arrangements are listed in Table 6 with corresponding T–ϕ–T′ angles. The first three range between 120° and 180°, and the remaining two are between 75° and 90°. The first three, most likely candidates for spanners between balls, are T(2D)–ϕ(4D)–T(2D) ≈ 176°, T(1D)–ϕ(3D)–T(1D) ≈ 125°, and T(1D)–ϕ(4D)–T(2D) ≈ 130°. All involve, beside the central linking ϕ, 2O(6) basal termini on each side.

Although the pathological part of the structure possesses twelve only partly occupied sites, assessing the potential-anion formal charges (and the anionic species) is possible by inspecting their coordinating cations. The ϕ(1D) and ϕ(6D) sites are approximately each half-occupied. The ϕ(1D) is coordinated by 2Y(2) and disordered 1T(1D) and 1K(1D). The X–ϕ(1D) distances are

larger than average, and we prefer to assign $\phi(1D) = OH^-$. The $\phi(6D)$ is coordinated by 2Y(2), and these distances are short. We suggest $\phi(6D) = OH^-$. The $\phi(4D)$ is coordinated by 2T(1D) + 2T(2D), but the individual cations are approximately half-population on average. We proposed $\phi(4D) = O^{2-}$. The $\phi(2D)$ is coordinated by T(2D) and the Na(3D) in the coordination cuboctahedron. Locally, if all sites were populated, the cluster would be $[Na(3D)\phi(5D)_4(T(2D)_2\phi(4D)\phi(2D)_2O(6)_4)_4]$, or $[Na(H_2O)_4(T_2O_7)_4]$. Since $\phi(5D)$ coordinates only to Na(3D), we suggest $\phi(5D) = H_2O$. The $\phi(2D)$ has site population much like T(2D), which is a bit lower than Na(3D). We suspect that these atoms—$\phi(2D)$, T(2D), and Na(3D)—are coupled together, and this means that $\phi(2D) = OH^-$. Finally, there is $\phi(3D)$. This is a possible T(1D)–$\phi(3D)$–T(1D) bridge. The $\phi(3D)$ population at this site is very uncertain, as seen in Table 3. With such uncertainties coupled with fragmentary evidence, $\phi(3D)$ could be O^{2-} [if both T(1D) are populated] or OH^- [if one T(1D) is populated] or H_2O [if both T(1D) are locally empty]. MSS assign $\phi(3D) = \frac{1}{2}(H_2O + O^{2-})$, $\frac{1}{2}(H_2O + OH^-)$, or $\frac{1}{2}(H_2O + H_2O)$, etc., where M assigns $\phi(3D) = O^{2-}$ as the bridging oxygen between two symmetry-related B cations in the T(1D) site. The ligand species proposed for each site ϕ is listed in Table 3.

Within the disordered whey, two clusters in the limit can be proposed: $[Na(H_2O)_4(T_2\phi_7)_4]$ for Na(3D) and $[KO_3(H_2O)(T\phi_4)]$ for K(1D) where the anionic unit is not specified for ϕ. This suggests that by other means, these units may be more precisely defined, but our X-ray diffraction experiments clearly cannot offer more than an averaged structure.

Chemical composition

Do the proposed occupancies in ashcroftine make any sense in light of Whitfield's chemical analysis in Table 1? As mentioned earlier, Y_2O_3 was discovered instead of Al_2O_3, and the presence of minor B_2O_3 was detected by M. From structure analysis and vapor-pressure measurement, the presence of substantial CO_2 must be accepted as a fact, and this was doubtless lost during ignition ($H_2O > 100$ °C) in Whitfield's analysis. From any point of view, a total analysis of ashcroftine would be exceedingly difficult even with contemporary techniques. Therefore, we elected to take the site occupancies of both studies in Table 3, reconstruct formulae, and compute contents as oxides.

From MSS, after balancing charge by adding requisite Ca^{2+} in place of Y^{3+}, for Z = 2 we get $K_{10.40}Na_{8.68}Y_{20.92}Ca_{3.08}Si_{54.16}O_{130.16}(OH)_{12.32}(CO_3)_{16.00}(H_2O)_{12.48}$. From M, after changing $1.88OH^-$ to $1.88H_2O$, the composition is $K_{10.00}Na_{10.80}Y_{20.56}Ca_{3.44}Si_{51.84}B_{4.16}O_{133.00}(OH)_{11.20}(CO_3)_{16.00}(H_2O)_{14.52}$. An "end-member" formula can be written: for Z = 4, $K_5Na_5Y_{12}(OH)_2(CO_3)_8(Si_{28}O_{70})\cdot 8H_2O$. Naturally, for such a complex substance with extensive disorder and other substituents, such a formula is only approximate.

Table 1 shows tolerable agreement between Whitfield's analysis and the structure results. Clearly, Ca^{2+} enters into the familiar solution with Y^{3+}. Note that the thermal parameters of MSS in Table 4 are larger than those of M, which indicates a lower mean atomic number than Y^{3+} at these sites. It is also evident that most H_2O (>100 °C) can be interpreted as (CO_2) in the structure, along with the smaller contributions made by $(OH)^-$, tightly bound (H_2O), etc.

It is interesting to note that neither structure study picked up all the water reported in Whitfield's analysis. Only about 76% total water reported was recovered, as detailed above. This suggests that much water in ashcroftine is disordered and undetectable by X-ray study. Considering the size of the giant ball, the possible content of zeolitic water could be quite substantial.

Dimensions of the truncated cuboctahedron (ball)

The crystal structures of at least five silicates and aluminosilicates that possess the t.c.o. as a fundamental building block are known. If a t.c.o. is constructed from plastic tetrahedra and Tygon tubings of equal length, the polyhedral skeleton is rigid and compact (i.e., minimal volume of circumsphere). The eight edges are removed, as discussed earlier for ashcroftine, and eight extra tetrahedra and eight extra bonds are inserted. The new polyhedron, which is not even semiregular, expands along the two principal directions a_1 and c. This is because the interior T–T–T angles are more obtuse, a consequence of the insertion of eight extra tetrahedra.

The distance between opposing octagonal facets was calculated. For an edge length l, we selected the sum of two Si–O distances, or Si–O–Si. Selecting d(Si–O) = 1.6 Å, l = 3.2 Å. The diameter (D) between octagonal faces is easy to derive: it is $D = 2(\frac{1}{2}l + 1/\sqrt{2}l + 1/\sqrt{2}l) = (2\sqrt{2} + 1)l = 3.828\ l$. For the ideal t.c.o., D = 12.2 Å for l = 3.2 Å.

Reasonably refined structures were used to calculate diameters between octagons and are discussed according to decreasing values of D. Ashcroftine is the only tetragonal structure, so we calculated $D(a_1)$ and $D(c)$ parallel to [100] and [001], respectively. From Figure 2, Si(2) evidently determines $D(a_1)$ and Si(3) determines $D(c)$. The values are $D(a_1)$ = 12.9 Å and $D(c)$ = 12.8 Å, respectively. If we put the average back into our equation for octagonal diameter of the t.c.o., we get T–O = 1.68 Å, a rather large value for an Si-O distance average. Clearly, the ball in ashcroftine is not strictly a semiregular t.c.o. In ashcroftine, OW(1) is the only identified species that occurs *within* the ball, and K(1) is next, being situated just outside the octagonal windows.

Linde zeolite A was refined by Pluth and Smith (1980). Here, Na(1) is just in the hexagonal faces, and Na(3) is inside the ball, displaced from the hexagonal window. Na(2) is on the octagonal faces. D = 12.3 Å for this structure.

The synthetic zeolite ZK-5 (Meier and Kokotailo, 1965) has Na^+ inside the ball. D = 12.1 Å for this structure.

Paulingite, solved and refined by Gordon et al. (1966), is a natural zeolite with an enormous cubic cell (a = 35.1

Å). All cations lie outside the ball. D = 12.0 Å for this structure.

The NH_4-rho zeolite (McCusker, 1984) is reminiscent of K(1) in ashcroftine: the NH_4^+ ion is in the plane of the octagonal window. D = 11.8 Å for this structure.

For the cubic zeolites, the range of four independent values is D = 11.8–12.3, with an average T–O = 1.57 Å. These values contrast with D = 12.9 Å and T–O = 1.68 Å for ashcroftine. No definite conclusions can be made about occupancies within the ball. In some structures, cations and/or water molecules have been located; in others, the ball is "empty," at least from X-ray studies. From the analytical data on ashcroftine, it is believed that the remaining water is present in the ball and that it is disordered at room temperature to the extent that X-ray diffraction experiments do not detect it, reminiscent of the extensive missing water in the giant pore or channel structure of cacoxenite (Moore and Shen, 1983).

Conclusion

Two reasonably refined crystal structures of the elephantine ashcroftine were obtained. At least 39 atoms occur in the asymmetric unit, and 12 of these are disordered. The fundamental building block is an ordered large ball, a broken truncated cuboctahedron, with tetragonal symmetry ($4/m\ 2/m\ 2/m$) and with composition $[Si_{48}O_{128}]$. The region between balls separated by ca. 4.0 Å along [001] is extensively disordered, and these balls have T–ϕ–T spanners between them. If we select T(1D)–ϕ(4D)–T(1D) as an ordered oligosilicate, the linking ϕ(4D), the associated O(6) from $[Si_{48}O_{128}]$, and ϕ(1D) [which also links to two encrusting Y(2)], the anhydrous $[Si_2O_7]$ spanner is created, or $^1_\infty[Si_{56}O_{140}]$, which becomes a tubular inosilicate with large bulbs oriented parallel to [001]. Adding all the ordered atoms in Table 3 together, we obtain $[K_8Na_2Y_{24}(OH)_4(CO_3)_{16}(Si_{56}O_{140})\cdot 10H_2O]^{10-}$. The charge is balanced by additional disordered alkali cations.

The $[Si_{48}O_{128}]$ ball includes O(1) to O(10). Of these, O(1), O(2), O(7), O(8), O(9), and O(10) knit the ball together by Si–O–Si bridges. These Si–O–Si angles are listed in Table 6 and range from 138° to 143°. They are essentially electrostatically neutral. The remaining O(3), O(4), O(5), and O(6) stick out from the ball to create a burr. These oxygens are electrostatically neutralized by Y(1), Y(2), K(1) and K(2) bonds. Only O(6), the broken segment of the t.c.o., links to the disordered tetrahedral cations, T(D). In fact, for the entire $^1_\infty[Si_{56}O_{140}]$, all terminal oxygens stick out like a burr such that the central pipe or tube has no vertices pointing into its domain. Yet again, the notion of the central ball as a template for the remainder of the structure is appealing.

Ashcroftine stands alone among the nepheline syenite secondary minerals in possessing an enormous silicate polyanion allied to the truncated cuboctahedron. A much smaller semiregular solid occurs in the nepheline syenite accessory tugtupite, as the $[Be_4Al_4Si_{16}O_{48}]$ truncated octahedron that defines the modular unit of a sodalite-type framework. We speculate that a cubic structure related to ashcroftine but with an isotropic distribution of crust or limbus around it may indeed exist as a late-stage nepheline syenite phase, associated with calcite, etc., and that the cubic symmetry may contribute to the elusive character of such a hypothetical phase.

Acknowledgments

Donation of *type* ashcroftine by the British Museum of Natural History and by the U.S. National Museum of Natural History is greatly appreciated. We cannot stress too much the importance of type material, and acknowledgement of such should not pass in silence.

P.B.M. appreciates support by the National Science Foundation (Grant EAR 84-08164) and the evident continued sympathy by that agency for his continued fascination and study of mineralogical monstrosities. P.K.S. wishes to thank the Tennessee computation facilities at the Tennessee Earthquake Information Center for use of their VAX computer.

S.M. acknowledges the Consiglio Nazionale delle Ricerche (Centro per lo studio della Geologia Dinamica e Strutturale dell'Appennino, Pisa) for financial support and the researchers at Centro per la Cristallografia Strutturale (Pavia) for their help in intensity-data collection.

References cited

Bethel, J.P., Ed. (1956) Webster's new collegiate dictionary (second edition), p. 488. G. and C. Merriam Co., Springfield, Massachusetts.

Britton, D., and Dunitz, J.D. (1973) A complete catalogue of polyhedra with eight or fewer vertices. Acta Crystallographica, A29, 362–371.

Gordon, E.K., Samson, S., and Kamb, W.B. (1966) Crystal structure of the zeolite paulingite. Science, 154, 1004–1007.

Gordon, S.G. (1924) Minerals obtained in Greenland on the second Academy-Vaux expedition, 1923. Proceedings of the Academy of Natural Sciences of Philadelphia, 76, 249–268.

Harris, D.M. (1981) The microdetermination of H_2O, CO_2 and SO_2 in glass using a 1280 °C microscope vacuum heating stage, cryopumping, and vapor pressure measurements from 77 to 273 K. Geochimica et Cosmochimica Acta, 45, 2023–2036.

Hey, M.H., and Bannister, F.A. (1933) Studies on the zeolites. Part IV. Ashcroftine (kalithomsonite of S.G. Gordon). Mineralogical Magazine, 23, 305–308.

Howells, E.R., Phillips, D.C., and Rogers, D. (1950) The probability distribution of X-ray intensity. II. Experimental investigation on the X-ray detection of center of symmetry. Acta Crystallographica, 3, 210–214.

Ibers, J.A., and Hamilton, W.C. (1974) International tables for X-ray crystallography, vol. 4, p. 99–100. Kynoch Press, Birmingham, England.

Laves, F. (1932) Zur Klassifikation der Silikate. Zeitschrift für Kristallographie, 82, 1–14.

Liebau, F. (1985) Structural chemistry of silicates: Structure, bonding and classification, p. 97–99. Springer-Verlag, New York.

Main, P., Woolfson, M.M., Lessinger, L., Germain, S., and Declerq, J.P. (1977) MULTAN 74, a system of computer programs for the automatic solution of crystal structures. University of York, England (1974).

Mandelbrot, B.B. (1983) The fractal geometry of nature, p. 74–83. W. H. Freeman and Co., New York.

McCusker, L.B. (1984) Crystal structures of the ammonium and hydrogen forms of zeolite rho. Zeolites, vol. 4, p. 51–55. Butterworth and Co. Ltd., London.

Meier, W.M., and Kokotailo, G.T. (1965) The crystal structure of synthetic zeolite ZK-5. Zeitschrift für Kristallographie, 121, 211–219.

Moore, P.B., and Shen, J. (1983) X-ray structural study of cacoxenite, a mineral phosphate. Nature, 306, 356–358.

Moore, P.B., Bennett, J.M., and Louisnathan, S.J. (1969) Ashcroftine is not a zeolite! Mineralogical Magazine, 37, 515–517.

Pluth, J.J., and Smith, J.V. (1980) Accurate redetermination of the crystal structure of dehydrated zeolite A. Absence of near zero coordination of sodium. Refinement of Si, Al-ordered superstructure. American Chemical Society Journal, 102, 4704–4708.

Manuscript received February 4, 1987
Manuscript accepted July 2, 1987